SCIENTIFIC REPORTS

SUBJECT AREAS:
PARASITE HOST RESPONSE
INFECTION
PARASITE BIOLOGY
MALARIA

Received
14 November 2012

Accepted
11 March 2013

Published
28 March 2013

Correspondence and requests for materials should be addressed to H.H. (hisa@med.gunma-u.ac.jp)

CD8$^+$ T cell activation by murine erythroblasts infected with malaria parasites

Takashi Imai[1], Hidekazu Ishida[2], Kazutomo Suzue[1], Makoto Hirai[1], Tomoyo Taniguchi[1,3], Hiroko Okada[1], Tomohisa Suzuki[1], Chikako Shimokawa[4] & Hajime Hisaeda[1]

[1]Department of Parasitology, Graduate School of Medicine, Gunma University, Gunma 371-8511, Japan, [2]Department of Microbiology and Immunology, Graduate School of Medical Sciences, Kyushu University, Fukuoka 812-8582, Japan, [3]Center for Medical Education, Faculty of Medicine, Gunma University, Gunma 371-8511, Japan, [4]Department of Parasitology, Institute of Tropical Medicine, Nagasaki University, Nagasaki 852-8523, Japan.

Recent studies show that some human malaria parasite species *Plasmodium falciparum* and *P. vivax* parasitize erythroblasts; however, the biological and clinical significance of this is unclear. To investigate further, we generated a rodent malaria parasite (*P. yoelii* 17XNL) expressing GFP-ovalbumin (OVA). Its infectivity to erythroblasts was confirmed, and parasitized erythroblasts were capable of initiating malaria infections. Experiments showed that MHC class I molecules were highly expressed on parasitized erythroblasts. As CD8$^+$ T cells recognize MHC class I and peptide complexes on target cells, and are involved in protection or pathology against malaria, we examined whether erythroblasts are targeted by CD8$^+$ T cells. Purified non-parasitized erythroblasts pulsed with OVA peptides were recognized by OVA-specific CD8$^+$ T cells. Crucially, parasitized erythroblasts isolated from GFP-OVA-, but not GFP- infected-mice, activated OT-I CD8$^+$ T cells, indicating that CD8$^+$ T cells recognize parasitized erythroblasts in an antigen-specific manner.

Malaria occurs throughout tropical and subtropical zones with 40% of the world's population at risk from the disease. Malaria affects approximately 300–500 million people, killing 1–3 million of them each year[1,2]. Malaria symptoms are caused by parasite multiplication within host erythrocytes and erythrocyte destruction causes anemia, one of the main clinical manifestations of the disease. Elimination of parasitized and non-parasitized erythrocytes can also occur via activation of the reticuloendothelial system[3,4] and acute malaria induces bone marrow suppression, resulting in a reduction in hematopoietic efficiency[5–7].

Malaria parasites normally parasitize mature erythrocytes and/or reticulocytes. Recently, however, both *P. falciparum* and *P. vivax* have been shown to invade erythroblasts *in vitro*[8,9], and parasitized erythroblasts were found within the bone marrow of patients with vivax malaria[10]. Infection of erythroblasts with malaria parasites is thought to cause anemia. However, the biological significance and pathological consequences of erythroblast infection by *Plasmodium* spp. remains unclear.

Little is known about erythroblast parasitism in rodent malaria parasites. We evaluated such parasitism using a mouse malaria model, through use of transgenic rodent malaria parasites that constitutively express GFP and OVA. Using fluorescence microscopy and flow cytometry, we confirmed that nucleated erythrocytes were parasitized in the bone marrow and spleen, where persistent hematopoiesis occurs in adult mice. The parasitized cells were infectious to malaria naive mice, and we found that the erythroblasts expressed substantial levels of MHC class I molecules, both before and after malaria infection. We also showed that erythroblasts pulsed with an antigenic epitope were recognized by specific CD8$^+$ T cells. Finally, we demonstrated that parasitized erythroblasts were recognized by CD8$^+$ T cells in an antigen-specific manner. These results are the first to demonstrate that rodent malaria parasites can parasitize erythroblasts and activate CD8$^+$ T cells. Our findings indicate that erythroblast parasitism might be a common feature of the host-parasite relationship in malaria.

Results

Generation of malaria parasites expressing GFP. We successfully generated a *P. yoelii* 17XNL line (PyNL) expressing GFP (PyNL-GFP) using a *Plasmodium* artificial chromosome (PAC) to investigate erythroblast parasitism in this rodent malaria line. GFP is expressed under the control of the elongation factor promoter

(Fig. 1a), which enables malaria parasites to express GFP during all of the erythrocytic stages of an infection. GFP expression in the transgenic parasite was detected by fluorescence microscopy in TER119$^+$ erythrocytes parasitized with mononuclear trophozoites and multinuclear schizonts (Fig. 1b, upper and lower panels, respectively). The parasite growth kinetics in mice infected with the transgenic parasite was similar to that observed for the wild-type parasite infections. The peak parasitemias and infection recovery times were comparable in both groups of mice (Fig. 1c), indicating that parasite pathogenicity was not adversely affected by genetic manipulation.

Detection of erythroblasts. Prior to examining PyNL parasitism of erythroblasts, we analyzed the phenotypic characteristics of erythroblasts to facilitate optimal detection. Almost all of the anucleate erythrocytes were removed after lysis in the peripheral blood, and the remaining lysis-resistant cells in the bone marrow were identified as nucleated cells. Thirty percent of the nucleated cell population consisted of TER119$^+$ cells (Supplementary Fig. 1a), which expressed CD71 (transferrin receptor), CD44 (adhesion molecule)[11] and MHC class I molecules. These molecules are typically expressed in erythroblasts, demonstrating that, after lysis, the TER119$^+$ cells were erythroblasts (Supplementary Fig. 1b).

Hematopoiesis occurs in both the bone marrow and spleen, even in adult mice. As the spleen plays important roles in eliminating parasitized erythrocytes and has pathological consequences for a malaria infection, we investigated the erythroblasts within this organ. CD44$^+$/MHC class I$^+$ erythroblasts were found within splenic tissue even after lysis, although their frequencies were low (Supplementary Fig. 1c, d). It should be noted that a substantial amount of TER119$^+$ nucleic acid$^+$ cells were present, even before lysis; these may have existed as lysis-susceptible cells and reticulocytes immediately after denucleation in the bone marrow or spleen. Induction of hemolytic anemia by administrating phenylhydrazine (PHZ), was found to increase the number of erythroblasts within the spleen possibly due to enhanced hematopoiesis (Supplementary Fig. 1c, d), suggesting that erythroblast numbers might increase during anemia-causing malaria attacks.

To confirm that the TER119$^+$ cells were erythroblasts and not reticulocytes (after lysis), fluorescence microscopic analysis was

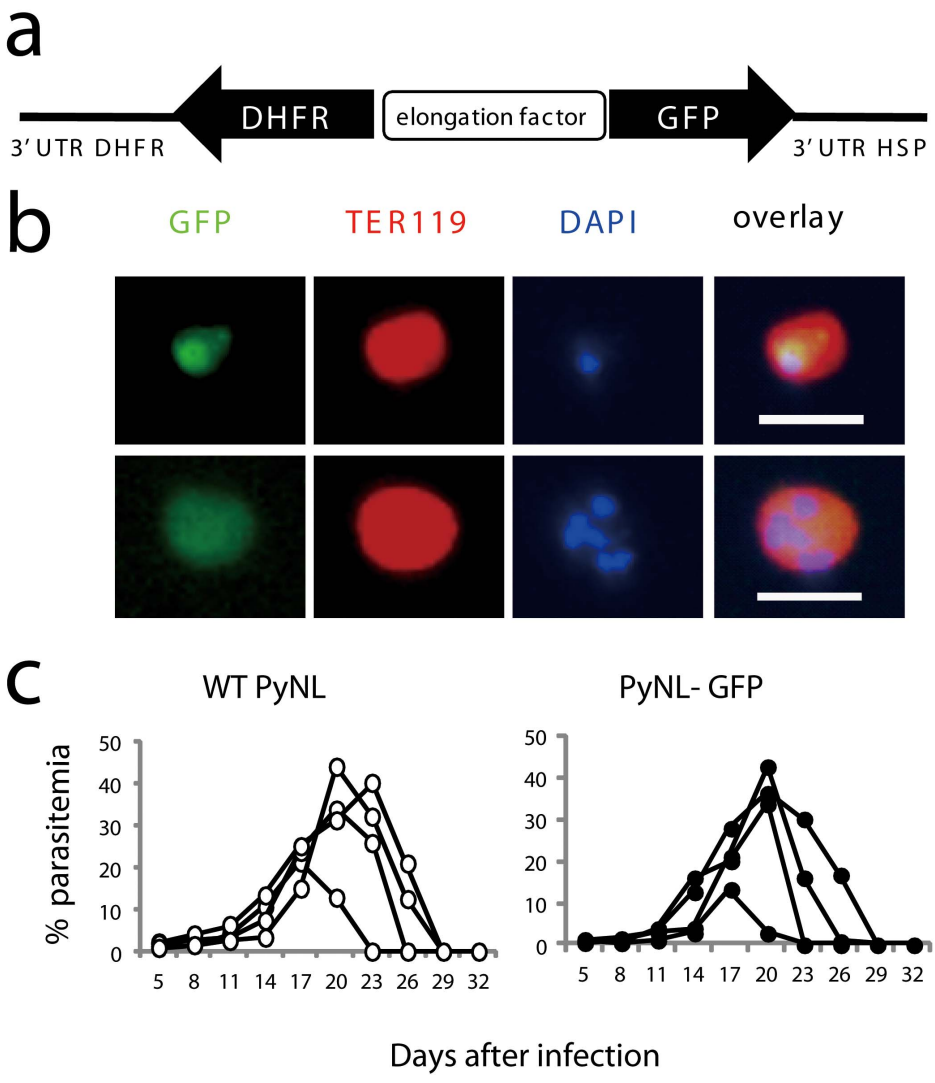

Figure 1 | Generation of recombinant *Plasmodium yoelii* 17XNL. (a) Construction of the *Plasmodium* artificial chromosome (PAC) containing GFP. PyNL parasites were transfected and recombinants were selected based on resistance to pyrimethamine conferred by exogenous expression of DHFR. (b) Detection of recombinant parasites using fluorescence microscopy. Peripheral blood from infected mice was stained with PE labeled anti-TER119 Ab and DAPI. Scale bars represent 10 μm. (c) Infectivity of recombinant parasites. C57BL/6 mice were intraperitoneally infected with WT or recombinant parasites (25000 parasitized erythrocytes). The time course of the parasitemia is shown. Each symbol indicates an individual mouse. Representative data from three independent experiments are shown.

performed. Although a few nucleated cells were observed in the sorted TER119$^+$ splenic cells from PHZ-treated mice before lysis, all TER119$^+$ cells were nucleated erythroblasts after lysis (Supplementary Fig. 1e). These nucleated TER119$^+$ cells expressed CD44 or CD71 (Supplementary Fig. 1f), and were consequently deemed to be erythroblasts.

Mouse malaria parasites parasitize nucleated erythroblasts. Using PyNL-GFP and the methods to distinguish erythroblasts described above, we were able to evaluate whether malaria parasites parasitize erythroblasts. TER119$^+$ cells were isolated from the peripheral blood, bone marrow, and spleens of mice infected (at around the peak parasitemia) with recombinant PyNL, and parasite GFP expression was detected. TER119$^+$ cells were nucleated erythroblasts after lysis. Although the majority of these cells lacked a GFP signal, TER119$^+$ GFP$^+$ cells were still clearly identified. TER119$^+$ GFP$^+$ cells contained parasite nuclei that co-localized with GFP and host cell nuclei, whilst the parasitized erythrocytes contained only parasite nuclei (Fig. 2a). These cells also expressed CD44 and CD71 (Fig. 2b, c), confirming that nucleated erythroblasts could be parasitized by malaria parasites. Although it was difficult to clearly distinguish the developmental stage of the parasites, multinucleated 'grape-like' parasites that were likely to be schizonts were observed (Fig. 2c). These observations indicate that the malaria parasites could multiply within the erythroblasts. Light microscopic analyses of Giemsa-stained preparations also indicated potential parasitism of the nucleated cells and some erythroblasts contained schizonts (Fig. 2d).

We next performed quantitative flow cytometric analyses. The percentage parasitemia of GFP$^+$ in TER119$^+$ cells within the peripheral blood was equivalent to that calculated based on microscopic examination of Giemsa-stained thin blood films (Fig. 3a, Fig. 3c), where 0.94 $\pm$ 0.54% or 20.41 $\pm$ 5.95% GFP$^+$ cells were detected 8 days or 18 days post-infection, respectively (Fig. 3b upper panel). The proportion of erythroblasts (TER119$^+$ cells/lysis-resistant cells) in the spleen increased dramatically (up to 30%) during the late stages of the infection (Fig. 3a), when mice suffered from high parasitemia and anemia (Fig. 3b lower panel). Such increases in the numbers of erythroblasts might be attributed to enhancement of erythropoiesis in the spleen to compensate for the anemia, as observed in the PHZ-treated mice (Supplementary Fig. 1c). GFP$^+$ erythroblasts were clearly detected within the spleen after lysis. Incidence of infection in splenic erythroblasts was 3.85 $\pm$ 0.96% in the early stage (Day 8), which was higher than that in the peripheral blood erythrocytes. Incidence in the late stage of the infection was 7.43 $\pm$ 2.55% (Day 18), which was lower than that in the peripheral blood (Fig. 3b upper panel).

We next analyzed the surface markers on the parasitized erythroblasts. In the peripheral blood, the parasitized GFP$^+$ erythrocytes expressed CD44 and were either negative or slightly positive for MHC class I (Fig. 3c). These phenotypes coincided with those of the reticulocytes, which are the preferred host cells for this parasite species[12]. The spleen and bone marrow contained GFP$^+$ cells with a similar phenotype to that observed in the peripheral blood before lysis. These cells were removed after lysis, and were thus considered to be contaminating reticulocytes from the peripheral blood. CD44$^+$/MHC class I^{hi} GFP$^+$ cells that were phenotypically distinct from the contaminating cells in the hemolyzed spleen and bone marrow were found to be parasitize erythroblasts (Fig. 3c). Expression of MHC class I molecules on parasitized erythroblasts was higher than that observed in non-parasitized erythroblasts in the infected mouse (mean fluorescence intercity [MFI], 1167 $\pm$ 261 vs 315 $\pm$ 46, day 20 or day 14 post infection, Fig. 3d, Fig. 4b). The GFP intensity in the infected erythroblasts was similar to that in infected reticulocytes and comprised two peaks (GFP^{hi} represents schizonts and GFP^{lo} represents trophozoites, Fig. 3c), suggesting that parasites grow in erythroblasts comparably in reticulocytes.

Parasitized erythroblasts are a potential source of infection. We observed parasite maturation and replication in erythroblasts; however, the number of schizonts appeared to be limited in number compared to what would normally be observed in reticulocytes. We next asked why erythroblast parasitism might be advantageous for malaria parasites. To confirm that new potentially invasive parasites had been generated within the parasitized erythroblasts, mice were transfused with GFP$^+$ MHC class I^{hi} parasitized erythroblasts isolated from the spleens of mice infected with PyNL-GFP (Fig. 4a, b). Infection of the mice with parasitized erythroblasts caused an elevation in parasitemia, and the kinetics of infection was similar to that seen using parasitized RBCs isolated from the peripheral blood of the same donor mice that the parasitized erythroblasts originated from (Fig. 4c). These data indicate that erythroblasts can support parasite growth and are a potential source of blood-stage infection.

Erythroblasts expressing MHC class I molecules are recognized by CD8$^+$ T cells. We and the others have previously reported that CD8$^+$ T cells are important for protection against blood stage malaria parasites[13–15]. On the other hand, there are some reports that CD8$^+$ T cells are pathogenic in murine experimental cerebral malaria[16,17]. In any case, CD8$^+$ T cells seem to be the important player in malaria infection. As shown above, the mouse malaria parasite could infect erythroblasts that have a high level of MHC class I molecules on their surface, suggesting that erythroblasts might be a target of CD8$^+$ T cells. To test this hypothesis, erythroblasts purified from PHZ-treated mouse spleens were pulsed with the OVA epitope (SIINFEKL), then co-cultured with CD8$^+$ T cells from the OT-I mice, before IFN-γ concentrations in the culture supernatants were measured (Fig. 5a). Expression level of MHC class I on erythroblasts was lower than that of splenocyte, higher than that of erythrocytes (Fig. 5b). We checked the expression level of H-2K^b and OVA CTL epitope complex on the surface of peptide pulsed erythroblasts or splenocytes (CD4 T cells). We found that H-2K^b and OVA CTL epitope complex positive cell in erythroblasts were fewer than that of CD4 T cells (Fig. 5c). Epitope-pulsed erythroblasts induced IFN-γ expression by CD8$^+$ T cells in a dose-dependent manner, although to a lesser extent than that exhibited by splenocytes (Fig. 5d). Response of OT-I CD8 T cells was abrogated in the presence of 25-D1.16 Ab that recognizes H-2K^b and OVA CTL epitope complex (Fig. 5e), clearly indicating requirement of interaction TCR and MHC class I/epitope complex for activation of CD8 T cells.

Next, we investigated whether erythroblasts were susceptible to the cytotoxicity exerted by CD8$^+$ T cells. Sorted erythroblasts were separated into two groups. One was pulsed with the OVA epitope and stained with green fluorescence (CFSE), while the other group was only stained with red fluorescence (PKH26). Cells were then cultured with OT-I CD8$^+$ T cells (effectors) as target cells or negative controls (Fig. 6a). Epitope-pulsed target cells were recognized by OT-I effector cells and were damaged as a result of the loss of membrane integrity; they were subsequently detected on the basis of PI-incorporation (Fig. 6b). These PI-stained cells were never observed in the presence of the CD8$^+$ T cells obtained from C57BL/6 mice (data not shown). In the absence of effector cells, the number of CFSE$^+$ erythroblasts was equal to the number of PKH26$^+$ cells in PI-excluded live cells. However, CFSE$^+$ erythroblasts decreased in a dose-dependent manner as the CFSE$^-$ PKH26$^-$ effector cells increased (Fig. 6c), indicating that target erythroblasts were susceptible to cytotoxicity. It should be noted that cytotoxicity against the erythroblasts was approximately two-fold lower than for the splenocytes (Fig. 6d). Response of OT-I CD8 T cells was abrogated by 25-D1.16 Ab (Fig. 6e). Together with the reduced ability of the

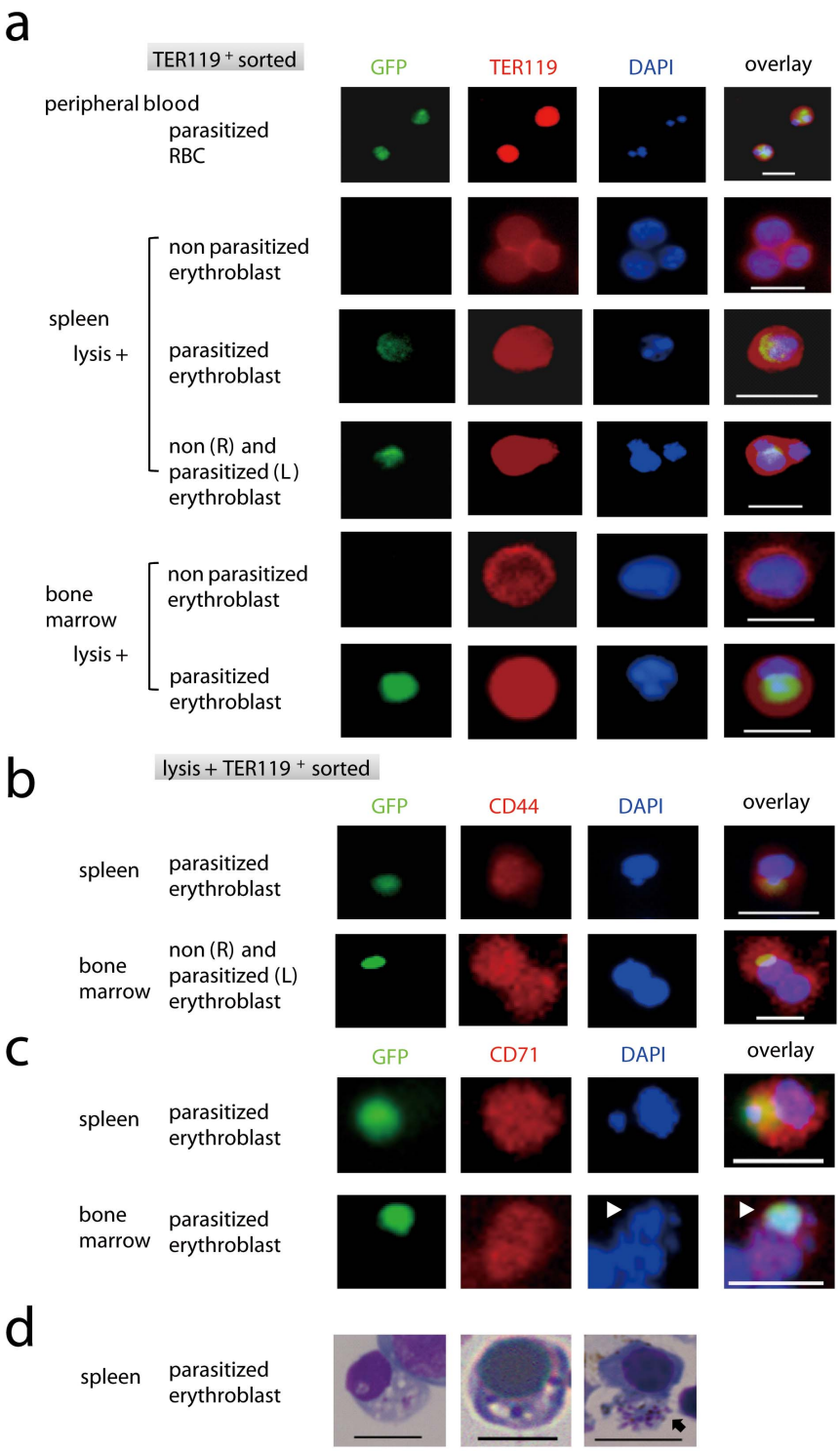

Figure 2 | ***Plasmodium yoelii*** **parasitism of mouse erythroblasts.** TER119$^+$ cells were sorted using MACS from the spleen and bone marrow samples from C57BL/6 mice 18 days after infection with PyNL-GFP. Cells stained with PE-conjugated anti-TER119 antibody (Ab) (a), PE-conjugated anti-CD44 Ab (b), anti-CD71 Ab (c), or DAPI, were analyzed by fluorescence microscopy. (d) Sorted cells were also stained with Giemsa solution. Scale bars represent 10 μm. Multi-nucleated 'grape-like' parasites likely to be schizonts (arrow head in c, arrow in d) were observed. Data comprise one representative of at least three independent experiments.

erythroblasts to induce IFN-γ expression by antigen-specific CD8$^+$ T cells, these results may explain the lower expression of MHC class I molecules when compared with splenocytes (Fig. 5b).

Parasitized erythroblasts activate CD8$^+$ T cells. Our data clearly indicate that erythroblasts are able to present antigen to CD8$^+$ T cells in conjunction with MHC class I molecules and induce IFN-γ production or cytotoxicity, thus prompting us to investigate antigen presentation by parasitized erythroblasts. To further utilize the OT-I CD8$^+$ T cells as an indicator for antigen presentation, the parasite lines PyNL-GFP and PyNL-GFP-OVA were generated. Expression of OVA protein within RBCs infected with the

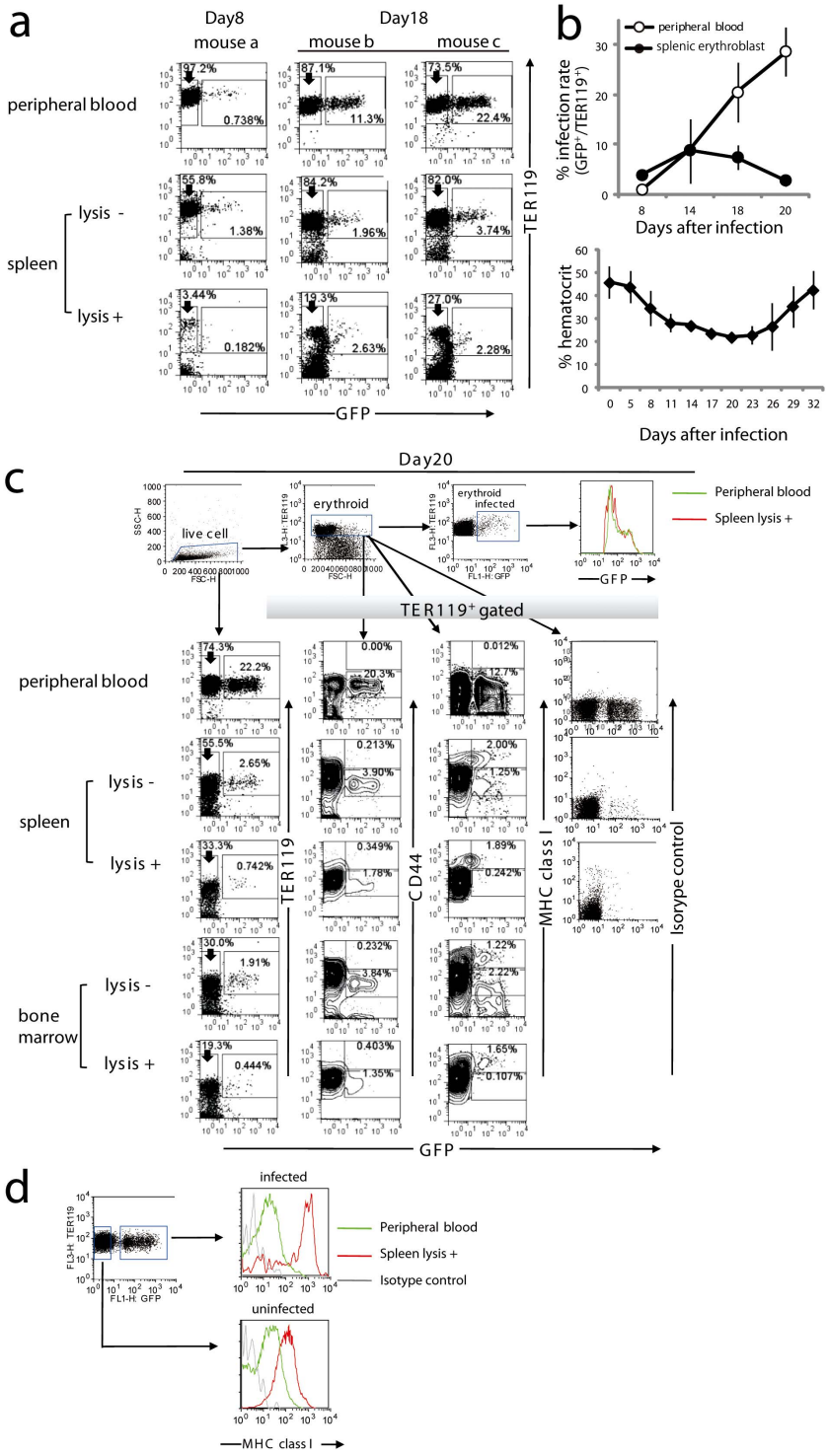

Figure 3 | Flow cytometric analyses of parasitized erythroblasts. C57BL/6 mice were infected with GFP-expressing malaria parasites. (a) Peripheral blood or spleen cells were stained with PE-Cy7 conjugated anti-TER119 Ab on day 8 and 18. Spleen cells were treated with or without lysis buffer before staining. Data are from one representative of at least four independent experiments. (b) The percentages of the GFP^+ cells within $TER119^+$ cells in the peripheral blood (parasitemia, open circles) and those in spleen cells after lysis (infected erythroblasts, closed circles) were calculated (upper panel). Data are mean ± SD from six mice. Hematocrits were evaluated to monitor anemia in mice infected with PyNL (lower panel). Data are ± SD from 10 mice. (c) Cells from the indicated organs on day 20 were stained with PE-Cy7 conjugated anti-TER119 Ab and PE-conjugated anti-CD44 Ab, or anti-MHC class I Ab. GFP expression in erythroblasts in mice infected with GFP-PyNL and the gating strategies (top panels). First, live cells were gated by forward scatter (FSC) and side scatter (SSC), then erythroid cells were gated as $TER119^+$ cells expression, and infected erythroid cells were gated as GFP^+ cells. A histogram shows GFP expression of erythrocytes (peripheral blood) and erythroblasts (lysed spleen cells) infected with GFP-PyNL. Cells after gating by FSC and SSC were analyzed for TER119 and GFP as in (a). Eythroid cells were analyzed for CD44, MHC class I, isotype control for MHC class I in right 3 columns. Numbers indicate percentage of boxed cells in gated population (not total cells). (d) Infected and uninfected erythroid cells were analyzed for expression of MHC class I. Data comprise one representative of three independent experiments.

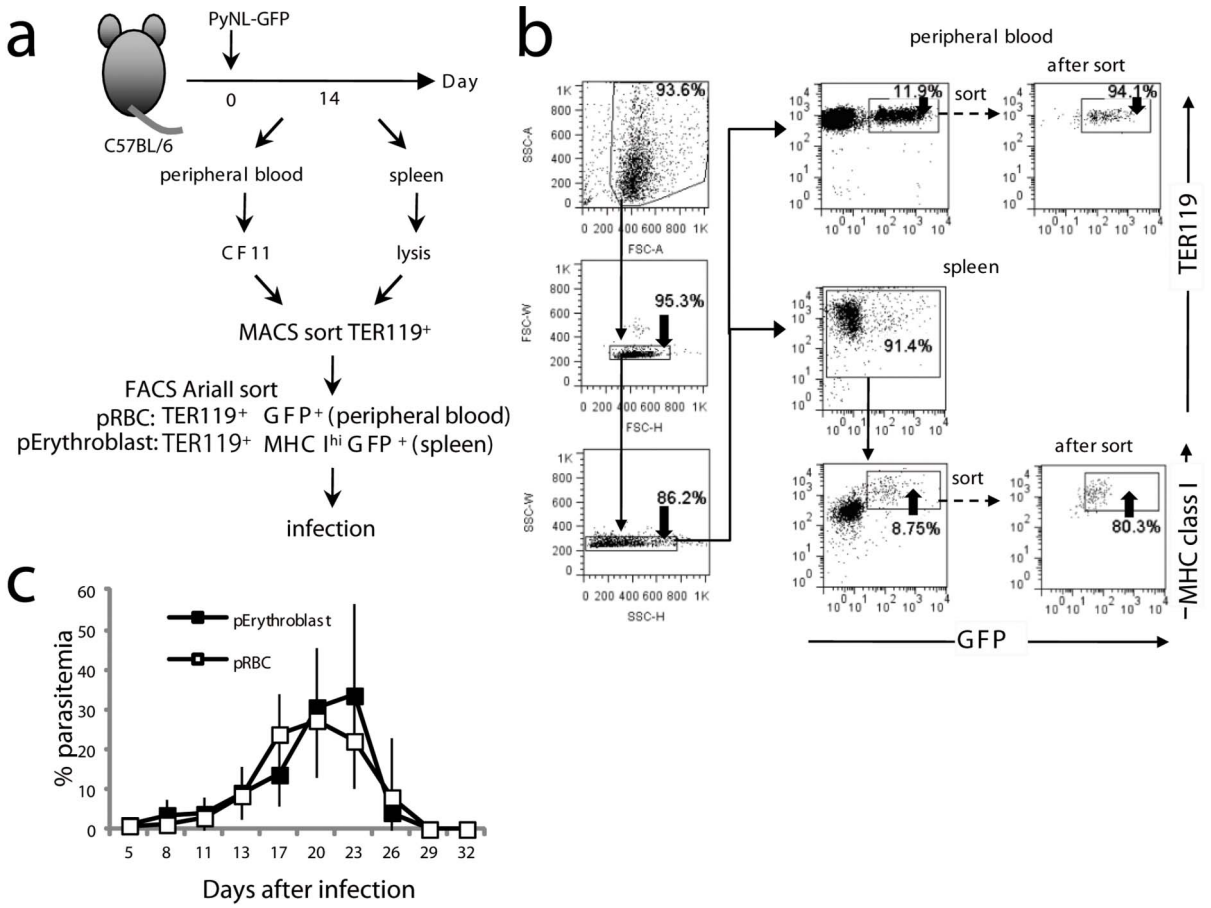

Figure 4 | Parasitized erythroblasts are a potential source of blood stage infection. (a) Protocol for challenge infection with parasitized erythroblasts (pErythroblasts). Peripheral blood was passed through a CF11 column to eliminate white blood cells then the TER119$^+$ RBCs were sorted. RBC lysed splenic TER119$^+$ erythroblasts were magnetically sorted 14 days after infection. (b) TER119$^+$ GFP$^+$ peripheral RBCs or TER119$^+$ MHC class I^{hi} GFP$^+$ splenic erythroblasts were purified by cell sorting. Mice were intravenously infected with 25,000 purified pRBCs or pErythroblasts. (c) Time course of parasitemia from pRBC injected mice (n = 9 mice, open square) or pErythroblast injected mice (n = 8 mice, closed square) (Mean ± S.D.). Representative data from two independent experiments are shown.

recombinant parasite was confirmed by western blot analysis (Fig. 7a, b). We first evaluated immunogenicity of the recombinant parasites. CD11c$^+$ DCs sorted from uninfected mice were cultured with OT-I CD8$^+$ T cells in the presence of soluble extracts from parasitized RBCs. Neither normal RBCs nor PyNL-GFP-parasitized RBCs induced production of IFN-γ from OT-I CD8$^+$ T cells. In contrast, addition of the PyNL-OVA-GFP-parasitized RBCs led OT-I cells to produce IFN-γ (Fig. 7c), indicating that exogenously expressed OVA in malaria parasites is immunogenic against OT-I T cells. Then, we investigated whether parasitized erythroblasts can present malarial antigens to CD8$^+$ cells. Mice were infected with PyNL-GFP or PyNL-GFP-OVA, and their splenic GFP$^+$ parasitized erythroblasts were purified and were fixed and co-cultured with OT-I CD8$^+$ T cells (Fig. 7d). GFP$^-$ uninfected erythroblasts could not induce IFN-γ production in OT-I cells. Parasitized erythroblasts isolated from mice infected with PyNL-GFP-OVA but not with PyNL-GFP could activate OT-I CD8$^+$ T cells (Fig. 7e). To exclude the possibility that contaminated DCs in erythroblast preparations activated OT-I cells, we voluntarily added DCs isolated from mice infected with PyNL-OVA-GFP. The addition of the DCs to erythroblasts did not affect the cytokine production of OT-I CD8$^+$ T cells (Fig. 7f). Thus, stimulatory features exerted by erythroblasts would not be affected if any DCs exist. These results clearly show that CD8$^+$ T cells recognize parasitized erythroblasts in an antigen-specific manner.

Discussion

Although human malaria parasites can parasitize erythroblasts, the biological and clinical significance of this phenomenon remains unclear. In this study, use of the PyNL-GFP transgenic line enabled us to demonstrate that rodent malaria parasites can also parasitize erythroblasts. Parasitized erythroblasts expressed MHC class I molecules on their surface that were recognized by antigen-specific CD8$^+$ T cells. Upon recognition, CD8$^+$ T cells secreted IFN-γ, which is essential for protection against malaria parasites.

Tamez and colleagues reported that the human malaria parasite, *P. falciparum* (Pf), parasitizes erythroblasts *in vitro*[8]. They found that as erythroblasts mature, they become more susceptible to Pf invasion[8]. Pf cell division was observed only in orthochromatic erythroblasts, the final precursor cells that form immediately before enucleation[8]. In our experiments, PyNL preferred to infect mature erythroblasts later than orthochromatic erythroblasts as judged by the CD44 expression patterns[11]. However, detailed analyses to define the relationship between the maturation stages of the erythroblasts and the susceptibility to infection are still required. The reason for parasite preference for the later stages of the erythroblast population might be due to the expression of receptor molecules on their surface ligated to merozoite molecules.

It is not clear if parasite invasion of erythroblasts could lead to formation of parasites that can re-infect RBCs. We confirmed that parasitized erythroblasts were able to parasitize RBCs to initiate new

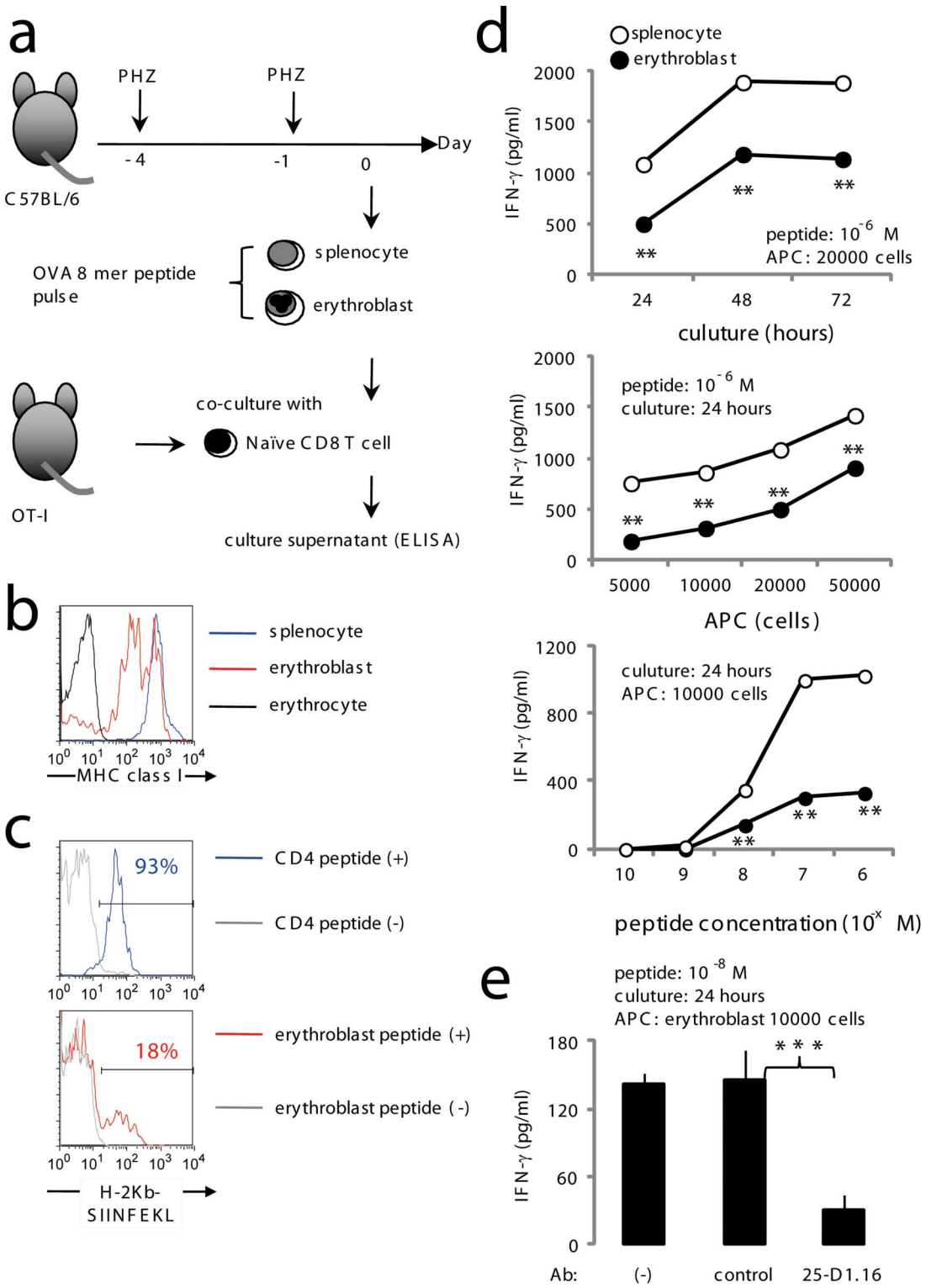

Figure 5 | CD8$^+$ T cell recognition of erythroblasts. (a) Protocols for the antigen presentation assay. Erythroblasts were isolated from spleen cells from C57BL/6 mice treated with 50 mg/kg weight PHZ on days −1 and −4. Cells were pulsed with the OVA epitope for 1 h followed by three extensive washes with culture medium before culturing with CD8$^+$ T cells from OT-I mice. Culture supernatants were collected for IFN-γ measurements using ELISA. (b) Expression of MHC class I on splenocytes, erythrocytes and erythroblasts are shown. (c) Expression of MHC class I-epitope complex on erythroblasts. Purified splenic CD4$^+$ T cells and erythroblasts were pulsed with or OVA epitope (SIINFEKL) and analyzed using 25-D1.16 Ab. Numbers indicate percentage of H-2K^b and OVA epitope complex positive cells in gated population. (d) Ten thousand or the indicated number of erythroblasts (closed circles) or splenocytes (open circles) pulsed with the OVA epitope were cultured with 1×10^5 OT-I CD8$^+$ T cells using the conditions indicated. (e) Abrogation of IFN-γ production due to blocking MHC/TCR interactions. OT-I cells and epitope-pulsed erythroblasts were cultured in the presence of 25-D1.16 or the control Ab. Concentration of IFN-γ in collected culture supernatants is shown. Data are shown as the mean ± S.D. from triplicate cultures of 3 mice. In d, e statistical significance is indicated as **$P < 0.01$ and ***$P < 0.01$. Representative data from 4–8 independent experiments are shown (a–e).

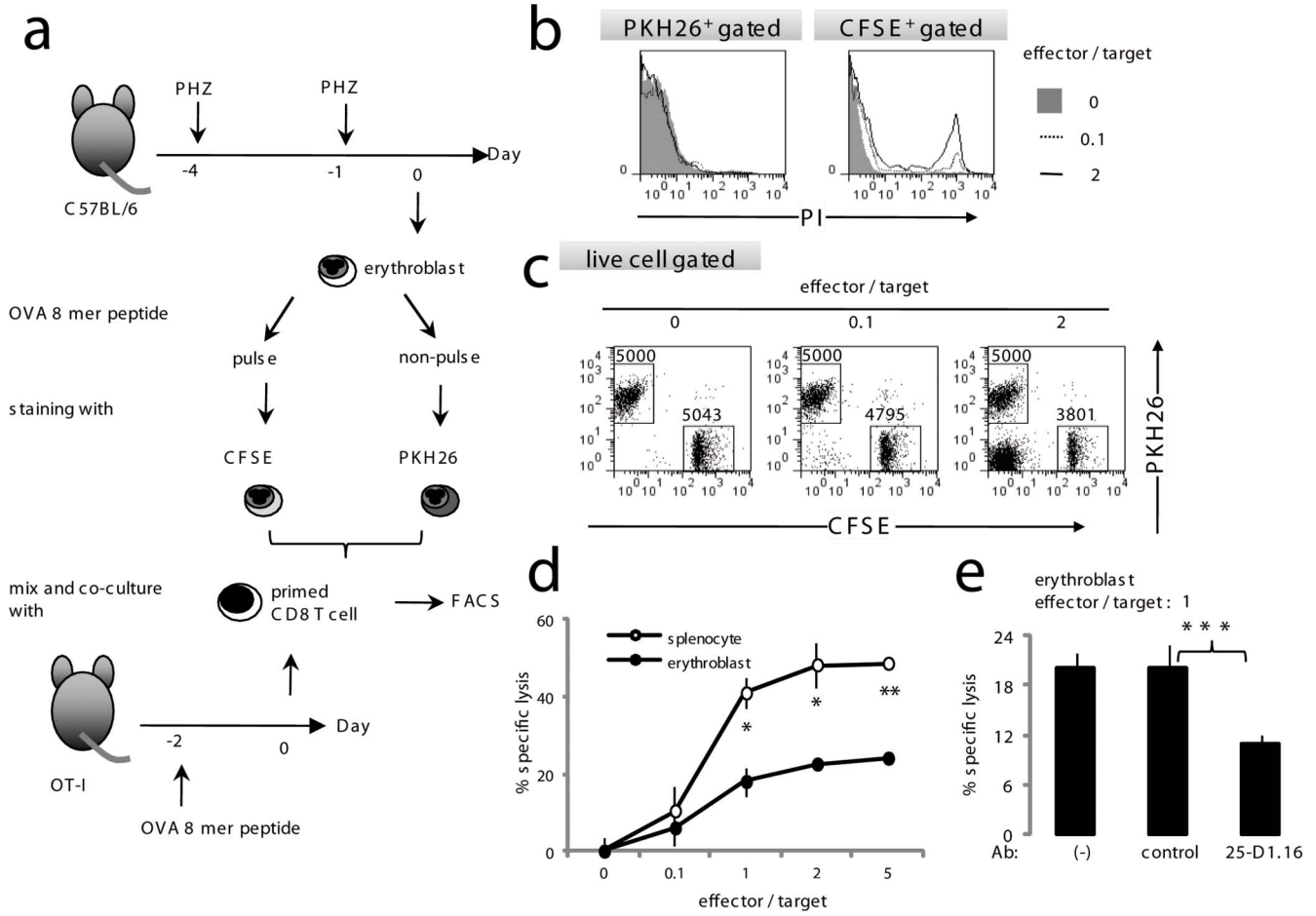

Figure 6 | Cytotoxicity by CD8$^+$ T cells against erythroblasts. (a) Protocols for the cytotoxicity assay. Erythroblasts or splenocytes were separated into two groups. One group was pulsed with 10^{-6} M OVA 8-mer peptide stained with CFSE. The other was only stained with PKH26. CFSE or PKH26 labeled cells were co-cultured for 4 h with variable numbers of primed CD8$^+$ T cells from the OT-I mice that had been injected with 20 nmol of the OVA 8-mer peptide without any adjuvants 2 days before the assay was commenced. After co-culturing at the ratio of OT-I cells indicated, the erythroblasts were stained with PI and analyzed using flow cytometry. (b) Incorporation of PI among CFSE$^+$ and PKH26$^+$ cells was demonstrated. (c) Cytotoxicity to erythroblasts by CD8$^+$ T cells was evaluated. OVA-pulsed CFSE$^+$ and OVA-free PKH26$^+$ cells were cultured with OT-I CD8$^+$ T cells at the effector/target ratio indicated. PI$^-$ live erythroblasts were plotted against CFSE and PKH26. The numbers of PKH26$^+$ or CFSE$^+$ cells are indicated in each panel. (d) OVA-specific cytotoxicity against splenocytes (open circles) or erythroblasts (closed circles) is represented. (e) Abrogation of cytotoxicity due to blocking MHC/TCR interactions. OT-I cells and 10^{-8} M OVA epitope-pulsed erythroblasts were cultured in the presence of 25-D1.16 or the control Ab. Cytotoxicity was calculated as the proportion of CFSE$^+$ surviving cells to PKH26$^+$ live cells. In d, e statistical significance is indicated as *$P < 0.05$, **$P < 0.01$ and ***$P < 0.01$. Representative data from 4 independent experiments are shown (a–e).

infections in mice. Infection of nucleated cells with malaria parasites is not as nonsensical as it might sound; avian malaria parasite species complete their whole blood-stage cycle in nucleated erythrocytes[18]. Thus, we suggest that erythroblast parasitism is not a 'dead-end' process but an important adaptation strategy for malaria parasites. Parasitized erythroblasts might confer resistance to host elimination mechanisms. It would be interesting to see what happens if we repeat these experiments using *P.chabaudi*, for example, where the murine host can control the primary peak parasitaemia, which is followed by the secondary appearance of the parasite[19]. It is quite possible that parasites remain in the erythroblast population post-peak when no parasites are visible in the peripheral blood using standard microscopy. Alternatively, parasitized erythroblasts may represent a dormant form of the parasite that has greater resistance to therapeutic agents[20], which might account for the recrudescence observed in individuals with Pf malaria after successful treatment with artemisinin-based drugs.

We confirmed that erythroblasts infected with PyNL expressed high levels of MHC class I molecules. However, the functional properties of these molecules on erythroblasts remain unknown, as no reports have directly demonstrated the antigen-presenting capacity of erythroblasts. We found that erythroblasts pulsed with an antigenic epitope were recognized by CD8$^+$ T cells, resulting in a lower induction of IFN-γ production and cytotoxic activities than for splenocytes. Furthermore, we demonstrated that parasitized erythroblasts activated CD8$^+$ T cells in an antigen-specific manner. Antigen presentation via class I molecules requires a supply of antigenic peptides resulting from proteolysis by proteasomes[21]. Experiments using proteasome inhibitors revealed protein degradation dependent on proteasomes in erythroblasts[22], suggesting that antigen processing does occur in erythroblasts. We speculate that parasite proteins are transported to the host cytosol or ER from the parasitophorous vacuole where they are processed and presented by the MHC class I.

We previously reported that CD8$^+$ T cells protect the host from blood-stage malaria primarily via secretion of IFN-γ, and the cytotoxic activity also contributes to protection[23]. One of the important functions of IFN-γ is up-regulation of MHC class I expression[24]. Although we did not evaluate whether or not erythroblasts have

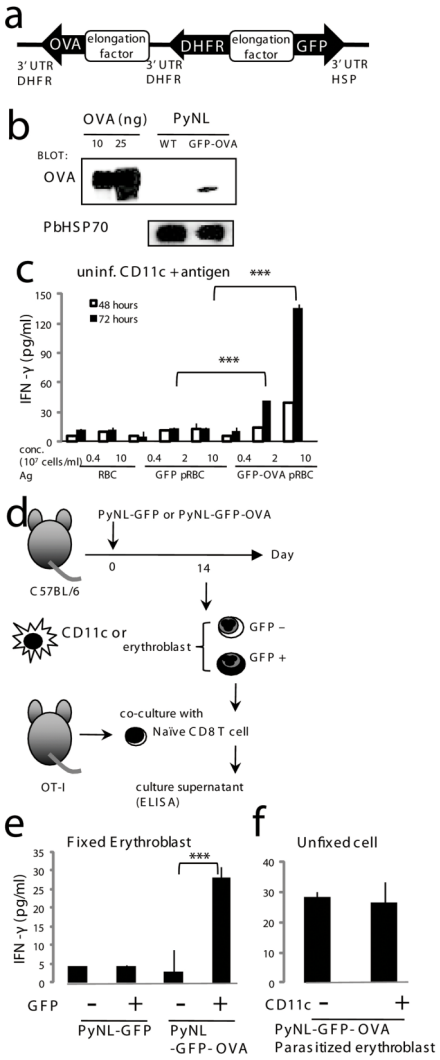

Figure 7 | Parasitized erythroblasts activate CD8$^+$ T cells. (a) Construction of the *Plasmodium* artificial chromosome (PAC) containing GFP and OVA. PyNL parasites were transfected and the recombinants selected based on resistance to pyrimethamine conferred by exogenous expression of DHFR. (b) Expression of OVA in the recombinant parasite was detected by western blot analysis. Protein extracts from parasitized RBCs purified from mice infected with the recombinant and parental (WT) parasite and OVA protein were separated on SDS-PAGE and transferred to nitrocellulose membranes followed by blotting with an anti-OVA antibody. An antibody against *P. berghei* HSP70 was used as an internal control. (c) Immunogenicity of OVA-expressing recombinant parasites. Purified CD11c$^+$ cells (2×10^4) from uninfected mice were co-cultured with 10^5 OT-I CD8$^+$ T cells in the presence of antigens from the indicated cells. (d) Protocol for antigen-specific recognition of parasitized erythroblasts. GFP$^+$ parasitized or GFP$^-$ uninfected erythroblasts isolated from spleen samples of C57BL/6 mice infected with PyNL-GFP or PyNL-GFP-OVA as shown in Fig. 4b. (e) Purified CD11c$^+$ cells (2×10^4) from C57BL/6 mice infected with the indicated parasite were pulsed with or without OVA peptide and fixed, then were co-cultured with 10^5 OT-I CD8$^+$ T cells. (f) Purified PyNL-GFP-OVA parasitized erythroblasts (2×10^4 cells) were mixed with or without CD11c$^+$ cells (2×10^4) from PyNL-GFP-OVA infected mouse and co-cultured with purified CD8$^+$ CD11c$^-$ T cells (10^5 cells) from Rag2$^{-/-}$ OT-I mice. (c, e, f) Activation of OT-I CD8$^+$ T cells was assessed by production of IFN-γ. Culture supernatants were collected after 72 hours otherwise mentioned, and the concentration of IFN-γ was measured. Mean ± S.D. from triplicate cultures from 4 mice is shown. Representative data from two to six independent experiments are shown. Statistical significance is indicated as *$P < 0.05$ and ***$P < 0.001$.

receptors for IFN-γ, nevertheless, erythroblasts are affected by IFN-γ[25]. Furthermore, we confirmed that expression of MHC class I on erythroblasts were upregulated by recombinant IFN-γ *in vitro* (Fig. S2). Expression of MHC class I molecules on parasitized erythroblasts was much higher than that of non-parasitized erythroblasts in infected mice (Fig. 3c, d and Fig. 4b); this might enable parasitized erythroblasts to be effectively recognized by CD8$^+$ T cells. Thus, it is quite possible that parasitized erythroblast killing is involved in CD8$^+$ T cell-mediated protection against malaria. However, killing of parasitized erythroblasts might play limited roles in overall protection to blood-stage malaria as most of parasites are found in reticulocytes or mature erythrocytes that could not be targeted of CD8$^+$ T cells. We postulate that the significance of erythroblast recognition implies reactivation of the primed CD8$^+$ T cells to produce IFN-γ, which in turn activates macrophages to effectively phagocytose parasitized reticulocytes and mature erythrocytes indifferently of MHC class I expression.

From a pathological point of view, erythroblast parasitism may partly contribute to the development of anemia, one of the major symptoms of malaria. Erythroblast parasitism, for example, may suppress erythropoiesis. Indeed, Tamez et al. reported that hematopoietic suppression-associated genes, such as *JUN* and *RARA*, were induced in Pf-parasitized erythroblasts[26]. Another possibility is that the destruction of parasitized erythroblasts caused by parasite growth and host immune responses reduces erythropoiesis, which is observed in other pathological situations. Parvovirus B19 infects erythroblasts and is the causative agent of pure red cell aplasia (PRCA). The marked decrease in erythroblast number observed after infection is a result of erythroblast destruction due to viral replication and the cytotoxic activity by CD8$^+$ T cells as a defense mechanism. Destruction of erythroblasts by self-reactive CD8$^+$ T cells is assumed to be the etiology of autoimmune PRCA[27]. Furthermore, Friend virus[28] infects erythroblasts, inducing tumorigenesis and resulting in the development of erythroleukemia. Reduction in the enlargement of the spleen containing massive virally transformed erythroblasts depends on CD8$^+$ T cells.

Our findings show that parasitism of erythroblasts by malaria parasites is an important aspect of malaria infection. Better understanding of the pathological and immunological aspects of malaria infection should provide new approaches for the effective control strategies. The blood-stage malaria is thought mostly to be controlled by humoral immunity. Blood-stage vaccines have been developed targeting antigens that expressed on parasites' surface, which are recognized by antibodies. Such molecules exposed to humoral immunity tend to be polymorphic, hampering development of effective vaccines. In contrast, CD8 T cells could recognize intracellular conserved antigens after antigen presentation. Thus, development of a malaria vaccine that activates CD8$^+$ T cells against blood-stage malaria might be hopeful.

Methods

Generation of malaria parasite lines expressing GFP and GFP-OVA. Blood-stage *Plasmodium yoelii* 17XNL (PyNL) was a generous gift from Dr. M. Torii (Ehime University). Recombinant PyNL was generated using a *Plasmodium* artificial chromosome (PAC)[29]. The following elements were inserted into the PAC: 1) elongation factor promoter; 2) green fluorescence protein (GFP); 3) Pb hsp70 3′ untranslated region; 4) *Plasmodium berghei* (Pb) pyrimethamine resistant gene dihydrofolate reductase-thymidyltransferase-ts (DHFR-ts) gene; 5) Pb DHFR-ts 3′ untranslated region (Fig. 1A); and 6) GFP-OVA, cytosolic form without the ovalbumin (OVA) signal sequence open reading frame (Fig. 6A). The elongation factor promoter facilitated PyNL gene expression during all of the erythrocytic stages. Transfection and drug selection have been described previously[30].

Mice and PyNL infection. C57BL/6 mice were obtained from SLC (Hamamatsu, Japan). Rag2$^{-/-}$ OT-I mice[31] were generous gifts from Dr. K. Yui (Nagasaki University). All mouse experiments were reviewed by the Committee for Ethics on Animal Experiments in the Faculty of Medicine, and carried out under the control of the Guidelines for Animal Experiments in the Faculty of Medicine, Gunma University, Japanese Law (No. 105) and Notification (No. 6) of the Government. PyNL-GFP or PyNL-GFP-OVA were obtained after fresh passage through a donor

mouse 3–4 days post-inoculation from frozen stock under drug pressure. Mice were infected with 25,000 parasitized red blood cells (pRBCs) intraperitoneally, unless otherwise indicated.

Determination of parasitemia and hematocrit. Blood samples were collected from experimental mice via the tail vein at the times indicated. Thin blood films were prepared and fixed with methanol followed by staining with Giemsa solution (Sigma, St. Louis, MO, USA). Parasitemia was determined by counting the percentage of pRBCs under a microscope, or by flow cytometry for mice infected with PyNL-GFP. Hematocrits were measured by centrifugation using a heparinized microhematocrit tube (Drummond microcaps; Drummond Scientific Company, Broomall, PA, USA).

Antibodies. PE-anti-TER119, APC-anti-TER119, PE-Cy7-anti-TER119, PE-anti-CD44, PE-anti-CD71, PE-anti-MHC class I and (PE)-anti-H-2K^b-SIINFEKL (25-D1.16) antibodies (eBioscience, San Diego, CA, USA) and FITC-anti GFP (abcam, Tokyo, Japan) were used for fluorescence microscopy or flow cytometry. Purified anti-CD16/32 (2.4G2) antibodies were also obtained from eBioscience. Anti-PE, anti-APC anti-CD11c and anti-CD8 microbeads (Miltenyi Biotech, Auburn, CA, USA) were used for magnetic cell-sorting (MACS) cell purification. Anti-IFN-γ capture and detection antibodies for enzyme-linked immunosorbent assays (ELISA) were obtained from R&D Systems (Minneapolis, MN, USA).

Erythroblast induction and purification. To stimulate erythroblast production *in vivo*, mice were injected intraperitoneally with 50 mg/kg weight of phenylhydrazine hydrochloride (PHZ, Kanto Chemical, Tokyo, Japan)[32,33]. To remove RBCs, the collected bone marrow or spleen cells were hemolyzed with ACK lysing buffer (NH_4Cl 8024 mg/l, $KHCO_3$ 1001 mg/l, EDTA $Na_2{\cdot}2H_2O$ 3.722 mg/l), or with 0.2% NaCl, and adjusted to natural osmotic pressure with 1.6% NaCl. Hemolyzed samples were washed twice with medium then incubated with anti-CD16/32 (Fc-block) and stained with PE- or APC-anti-TER119 antibodies. Anti-PE or anti-APC microbeads were then added to the samples and the erythroblasts purified using MACS. Purified erythroblasts were used for flow cytometry, fluorescence microscopy, antigen presentation, and cytotoxicity assays. The sorted bone marrow or splenic erythroid precursor cell (TER119$^+$ cell) purity was > 90–95%. Parasitized erythroblasts were isolated from enriched erythroblasts from mice infected with PyNL-GFP-GFP or PyNL-GFP-OVA after further staining with PE-anti-MHC class I antibodies. GFP$^-$TER119$^+$ and GFP$^+$MHC class I^{hi} cells were sorted using a FACSAria II cell sorter (Becton Dickinson, Mountain View, CA, USA) and used as non-parasitized and parasitized erythroblasts, respectively.

Flow cytometry and fluorescence microscopy. Peripheral blood, bone marrow and spleen cell suspensions, treated with or without lysing buffer, were incubated with Fc-block and stained with fluorochrome-labeled antibodies. Stained cells were analyzed using FACSCalibur flow cytometry (Becton Dickinson, Mountain View, CA, USA); data were analyzed using FlowJo software (Treestar, Ashland, OR, USA). Stained samples were fixed with 0.5% paraformaldehyde, smeared with cytospin 4 cytocentrifuge (Thermo Fisher Scientific, Waltham, MA, USA), then mounted with VECTASHIELD Mounting Medium and DAPI (Vector Laboratories, Burlingame, CA, USA). Samples were analyzed using a BIOREVO BZ-9000 microscope (KEYENCE, Osaka, Japan). Data were analyzed with BZ-II software (KEYENCE).

Antigen presentation assays. Splenic erythroblasts and TER119$^-$ splenocytes (1×10^7 cells/ml) were pulsed with 10^{-6} M or the indicated dose of the OVA 8-mer CTL epitope (SIINFEKL) for 1 h at 37°C. Cells were washed three times with RPMI 1640 (Sigma). For MHC class I blocking experiment (Fig. 5e), cells were Fc-blocked and incubated with 1 μg/ml of anti-H-2K^b-SIINFEKL (25-D1.16) or control Abs for 30 min at 4°C, then washed with PRMI-1640. Cells were fixed by 0.5% para-formaldehyde and quenched by 0.1 M glycine, as standard method in antigen presentation assay[34]. Erythroblasts or TER119$^-$ splenocytes (2×10^4 or the indicated number) were co-cultured with purified Rag2$^{-/-}$ OT-I CD8$^+$ CD11c$^-$ T cells (10^5) in a 200 μl final volume in a 96-well plate for 48–76 h or as indicated at 37°C in a CO_2 incubator with RPMI 1640 (Sigma) containing 10% fetal bovine serum, 2 mM L-glutamine, 1 mM sodium pyruvate, 0.1 mM non-essential amino acids, penicillin-streptomycin and 2-mercaptoethanol. Culture supernatants were collected to measure the IFN-γ released from CD8$^+$ T cells using ELISA.

Cytotoxicity assays. *In vitro* cytotoxicity assays were performed using VITAL[35]. Briefly, splenic erythroblasts or TER119$^-$ splenocytes were separated into two groups. One group (1×10^7 cells/ml) was pulsed with 10^{-6} M OVA 8-mer peptide for 1 h at 37°C in a CO_2 incubator then stained with 250 nM 5-(and-6)-carboxyfluorescein diacetate, succinimidyl ester (CFSE, Molecular Probes, Invitrogen, Eugene, OR, USA) for 5 min at room temperature. The other group (1×10^7 cells/ml) was stained with 2 μM PKH26 (Sigma) for 4 min at room temperature. Dead cells were removed from CFSE or PKH26 labeled cells using Lympholyte-M (Cedarlane Laboratories, Ontario, Canada). Living CFSE or PKH26 labeled cells were co-cultured for 4 h at 37°C in a CO_2 incubator with or without a variable number of primed CD8$^+$ T cells from OT-I mice that had been injected with 20 nmol of the OVA 8-mer peptide two days before the assay commenced. After co-culturing at the indicated ratio of OT-I cells, samples were stained with PI and analyzed using a flow cytometer. PI$^-$ cells were gated, and the mean percent survival of peptide pulsed target cells (CFSE$^+$) was calculated relative to non-pulsed target cells (PKH26$^+$). For MHC class I blocking experiment (Fig. 6e), cells were Fc blocked and co-cultured with 1 μg/ml of anti-H-2K^b-SIINFEKL (25-D1.16) or control Abs. All data were adjusted according to the following formula: % survival = 100 × CFSE$^+$ cell number/PKH26$^+$ cell number (5000 cells), % specific lysis = 100 – % survival.

Statistical analysis. Statistical evaluation of differences between the experimental groups was conducted using analysis of variance and two-tailed unpaired Student's t tests. $P < 0.05$ was considered statistically significant.

1. Snow, R. W., Guerra, C. A., Noor, A. M., Myint, H. Y. & Hay, S. I. The global distribution of clinical episodes of Plasmodium falciparum malaria. *Nature* **434**, 214–217 (2005).
2. Good, M. F., Xu, H., Wykes, M. & Engwerda, C. R. Development and regulation of cell-mediated immune responses to the blood stages of malaria: implications for vaccine research. *Annu Rev Immunol* **23**, 69–99 (2005).
3. Waitumbi, J. N., Opollo, M. O., Muga, R. O., Misore, A. O. & Stoute, J. A. Red cell surface changes and erythrophagocytosis in children with severe plasmodium falciparum anemia. *Blood* **95**, 1481–1486 (2000).
4. Abdalla, S. H. Peripheral blood and bone marrow leucocytes in Gambian children with malaria: numerical changes and evaluation of phagocytosis. *Ann Trop Paediatr* **8**, 250–258 (1988).
5. Haldar, K. & Mohandas, N. Malaria, erythrocytic infection, and anemia. *Hematology Am Soc Hematol Educ Program*, 87–93 (2009).
6. Chang, K. H. & Stevenson, M. M. Malarial anaemia: mechanisms and implications of insufficient erythropoiesis during blood-stage malaria. *Int J Parasitol* **34**, 1501–1516 (2004).
7. Chang, K. H., Tam, M. & Stevenson, M. M. Inappropriately low reticulocytosis in severe malarial anemia correlates with suppression in the development of late erythroid precursors. *Blood* **103**, 3727–3735 (2004).
8. Tamez, P. A., Liu, H., Fernandez-Pol, S., Haldar, K. & Wickrema, A. Stage-specific susceptibility of human erythroblasts to Plasmodium falciparum malaria infection. *Blood* **114**, 3652–3655 (2009).
9. Panichakul, T. *et al.* Production of erythropoietic cells in vitro for continuous culture of Plasmodium vivax. *Int J Parasitol* **37**, 1551–1557 (2007).
10. Ru, Y. X. *et al.* Invasion of erythroblasts by Pasmodium vivax: A new mechanism contributing to malarial anemia. *Ultrastruct Pathol* **33**, 236–242 (2009).
11. Chen, K. *et al.* Resolving the distinct stages in erythroid differentiation based on dynamic changes in membrane protein expression during erythropoiesis. *Proc Natl Acad Sci U S A* **106**, 17413–17418 (2009).
12. Otsuki, H. *et al.* Single amino acid substitution in Plasmodium yoelii erythrocyte ligand determines its localization and controls parasite virulence. *Proc Natl Acad Sci U S A* **106**, 7167–7172 (2009).
13. Weidanz, W. P., Melancon-Kaplan, J. & Cavacini, L. A. Cell-mediated immunity to the asexual blood stages of malarial parasites: animal models. *Immunol Lett* **25**, 87–95 (1990).
14. Podoba, J. E. & Stevenson, M. M. CD4$^+$ and CD8$^+$ T lymphocytes both contribute to acquired immunity to blood-stage Plasmodium chabaudi AS. *Infect Immun* **59**, 51–58 (1991).
15. Lundie, R. J. *et al.* Blood-stage Plasmodium infection induces CD8$^+$ T lymphocytes to parasite-expressed antigens, largely regulated by CD8alpha+ dendritic cells. *Proc Natl Acad Sci U S A* **105**, 14509–14514 (2008).
16. Lau, L. S. *et al.* Blood-Stage Plasmodium berghei Infection Generates a Potent, Specific CD8$^+$ T-Cell Response Despite Residence Largely in Cells Lacking MHC I Processing Machinery. *J Infect Dis* **204**, 1989–1996 (2011).
17. Howe, L. *et al.* Malaria parasites (Plasmodium spp.) infecting introduced, native and endemic New Zealand birds. *Parasitol Res* **110**, 913–923 (2012).
18. Stephens, R., Culleton, R. L. & Lamb, T. J. The contribution of Plasmodium chabaudi to our understanding of malaria. *Trends Parasitol* **28**, 73–82 (2012).
19. LaCrue, A. N., Scheel, M., Kennedy, K., Kumar, N. & Kyle, D. E. Effects of artesunate on parasite recrudescence and dormancy in the rodent malaria model Plasmodium vinckei. *PLoS One* **6**, e26689 (2011).
20. Dondorp, A. M. *et al.* Artemisinin resistance in Plasmodium falciparum malaria. *N Engl J Med* **361**, 455–467 (2009).
21. Groettrup, M. *et al.* A role for the proteasome regulator PA28alpha in antigen presentation. *Nature* **381**, 166–168 (1996).
22. Chen, C. Y., Pajak, L., Tamburlin, J., Bofinger, D. & Koury, S. T. The effect of proteasome inhibitors on mammalian erythroid terminal differentiation. *Exp Hematol* **30**, 634–639 (2002).
23. Imai, T. *et al.* Involvement of CD8$^+$ T cells in protective immunity against murine blood-stage infection with Plasmodium yoelii 17XL strain. *Eur J Immunol* **40**, 1053–1061 (2010).
24. Zhou, F. Molecular mechanisms of IFN-gamma to up-regulate MHC class I antigen processing and presentation. *Int Rev Immunol* **28**, 239–260 (2009).
25. Felli, N. *et al.* Multiple members of the TNF superfamily contribute to IFN-gamma-mediated inhibition of erythropoiesis. *J Immunol* **175**, 1464–1472 (2005).
26. Tamez, P. A., Liu, H., Wickrema, A. & Haldar, K. P. falciparum Modulates Erythroblast Cell Gene Expression in Signaling and Erythrocyte Production Pathways. *PLoS One* **6**, e19307 (2011).
27. Fisch, P., Handgretinger, R. & Schaefer, H. E. Pure red cell aplasia. *Br J Haematol* **111**, 1010–1022 (2000).

28. Takamura, S. *et al.* Premature terminal exhaustion of Friend virus-specific effector CD8$^+$ T cells by rapid induction of multiple inhibitory receptors. *J Immunol* **184**, 4696–4707 (2010).
29. Iwanaga, S. *et al.* Functional identification of the Plasmodium centromere and generation of a Plasmodium artificial chromosome. *Cell Host Microbe* **7**, 245–255 (2010).
30. Janse, C. J., Ramesar, J. & Waters, A. P. High-efficiency transfection and drug selection of genetically transformed blood stages of the rodent malaria parasite Plasmodium berghei. *Nat Protoc* **1**, 346–356 (2006).
31. Miyakoda, M. *et al.* Malaria-specific and nonspecific activation of CD8$^+$ T cells during blood stage of Plasmodium berghei infection. *J Immunol* **181**, 1420–1428 (2008).
32. Vannucchi, A. M. *et al.* Identification and characterization of a bipotent (erythroid and megakaryocytic) cell precursor from the spleen of phenylhydrazine-treated mice. *Blood* **95**, 2559–2568 (2000).
33. Socolovsky, M. *et al.* Ineffective erythropoiesis in Stat5a$^{-/-}$5b$^{-/-}$ mice due to decreased survival of early erythroblasts. *Blood* **98**, 3261–3273 (2001).
34. Imai, T. *et al.* Heat shock protein 90 (HSP90) contributes to cytosolic translocation of extracellular antigen for cross-presentation by dendritic cells. *Proc Natl Acad Sci U S A* **108**, 16363–16368 (2011).
35. Hermans, I. F. *et al.* The VITAL assay: a versatile fluorometric technique for assessing CTL- and NKT-mediated cytotoxicity against multiple targets in vitro and in vivo. *J Immunol Methods* **285**, 25–40 (2004).

Acknowledgments

We thank Dr. Shiroh Iwanaga for his help in generating the PAC. This study was supported by grant-in-aid (24117504 to H.H., 24790399 to T.I.) and the Strategic Fund for the Promotion of Science and Technology to H.H. from the Ministry of Education, Culture, Sports, Science and Technology of Japan and the Ministry of Health, Labour and Welfare of Japan (H24-Shitei-004) to H.H., and a Research Grant for Basic Medical Sciences from the Gunma Medical Association to T.I, and the Takeda Memorial Foundation to H.H., and Gunma University Operational Grants for multi-drug resistance to H.H.

Author contributions

Contribution: T.I. performed the experiments, analyzed the results, created the figures, and wrote the manuscript; H.I. and M.H. generated the recombinant parasites; K.S. analyzed the results; T.T., H.O., T.S. and C.S. performed the experiments; and H.H. directed the project, analyzed the results and wrote the manuscript.

Additional information

Supplementary information accompanies this paper at http://www.nature.com/scientificreports

Competing financial interests: The authors declare no competing financial interests.

How to cite this article: Imai, T. *et al.* CD8$^+$ T cell activation by murine erythroblasts infected with malaria parasites. *Sci. Rep.* **3**, 1572; DOI:10.1038/srep01572 (2013).